In-oribt selection of cryocooler drive frequencies for XRISM/*Resolve*

Gary A. Sneiderman*[a], Meng P. Chiao[a], Caroline A. Kilbourne[a],
F. Scott Porter[a], Masahiro Tsujimoto[b]
[a]NASA, Goddard Space Flight Center, Greenbelt, MD 20771 USA; [b]Institute of Space and Astronautical Science, JAXA, 3-1-1 Yoshinodai, Chuo-ku, Sagimahara, Kanagawa 252-5210, Japan

ABSTRACT

The XRISM/*Resolve* instrument cooling system uses adiabatic demagnetization refrigerators (ADRs) to cool the detectors to 50 mK and Joule-Thomson and Stirling cryocoolers to reduce heat load on the He tank supporting the ADRs. *Resolve* was designed with tunable cryocooler drive frequencies so that interference could be avoided. The cryocooler generated micro-vibration changes with drive frequency and that micro-vibration causes interference and degrades instrument performance. Poor drive frequency choices have been shown to dramatically impact ADR cooling power, temperature stability, detector noise, and degrading spectroscopic performance. However, some choices are free of these features, allowing the instrument to satisfy its performance requirements with significant margin. Thus, the choice of drive frequencies is critical to achieving peak instrument performance. The drive frequencies of the Joule-Thomson cooler, near 52 Hz, and the Stirling coolers, near 15 Hz, were adjusted in three scan sequences while measuring interference to narrow candidate frequency options. Choices were based on stability of the 50 mK control thermometer, changes in the ADR demagnetization rate, and changes in detector noise. These scans were performed routinely during ground testing. Surprisingly though, the results were not repeatable after the Dewar was warmed and re-cooled but were repeatable when remeasured during the same test campaign. Since the good/bad drive frequencies change during Dewar warmup/cooldown, and possibly after vibration events, the drive frequencies could not be finalized before launch. This paper describes the cryocooler frequency scan measurements and compares the results during instrument commissioning to those performed during ground tests.

Keywords: XRISM, x-ray microcalorimeter, microphonic, cryocooler drive frequency selection

1. INTRODUCTION

Many spaceborne telescopes are sensitive to on-board sources of vibration and mitigating that vibration to achieve the required instrument sensitivity is a difficult multi-disciplinary systems-engineering challenge. For imaging telescopes, on-board vibration can cause image blur, and for *Resolve's* cryogenic microcalorimeters it manifests as heat or induces microphonic noise, both of which degrade spectrographic sensitivity. While the consequence of on-board vibration is unique to each instrument design, the problems are similar and so too are many of the solutions. This paper describes the approach taken to mitigate exported vibration with examples and lessons to serve as reference for future missions.

The XRISM mission[1] was launched into Low-Earth Orbit on September 7, 2023 and hosts *Resolve*[2], a high-resolution microcalorimeter spectrometer featuring a 36 pixel detector array operated at 50 mK that has achieved extraordinary energy resolution[3].

Resolve can measure the tiny amount of heat from each x-ray focused onto one of its 36 pixels so long as the detectors are cold enough, a small fraction of a degree above absolute zero. The Adiabatic Demagnetization Refrigerators (ADRs)[4] and their controllers, the ADR Controller or ADRC[5], cool the detectors to 50 mK and sustain them precisely at that temperature by controlling the demagnetization rate of the ADR magnets using a PID controller and feedback from one of the germanium resistance thermometers located near the detectors. *Resolve* can maintain stable 50 mK operation for periods of almost two days before needing to recycle the ADRs and re-stabilize back at 50 mK, a process that takes about an hour.

*gary.a.sneiderman@nasa.gov; phone 1 240 447-0588

The *Resolve* cooling system and detector system[6] were integrated to the Dewar[7] and hermetically sealed and pumped down to high vacuum early in the Project schedule. Then the system was tested at operational temperatures in ten campaigns prior to launch. The cooling system includes a Joule Thompson cryocooler (JT); four double-stage Stirling cryocoolers (2ST) one pair as shield coolers (SC-A and SC-B) and the other pair as pre-coolers (PC-A and PC-B) for the JT; >30 L of superfluid helium; and three ADRs.

The *Resolve* instrument is the collaborative product of NASA/Goddard Space Flight Center and JAXA with contributions from SRON and ESA. The *Resolve* block diagram indicating the international contributions is shown in Figure 1.

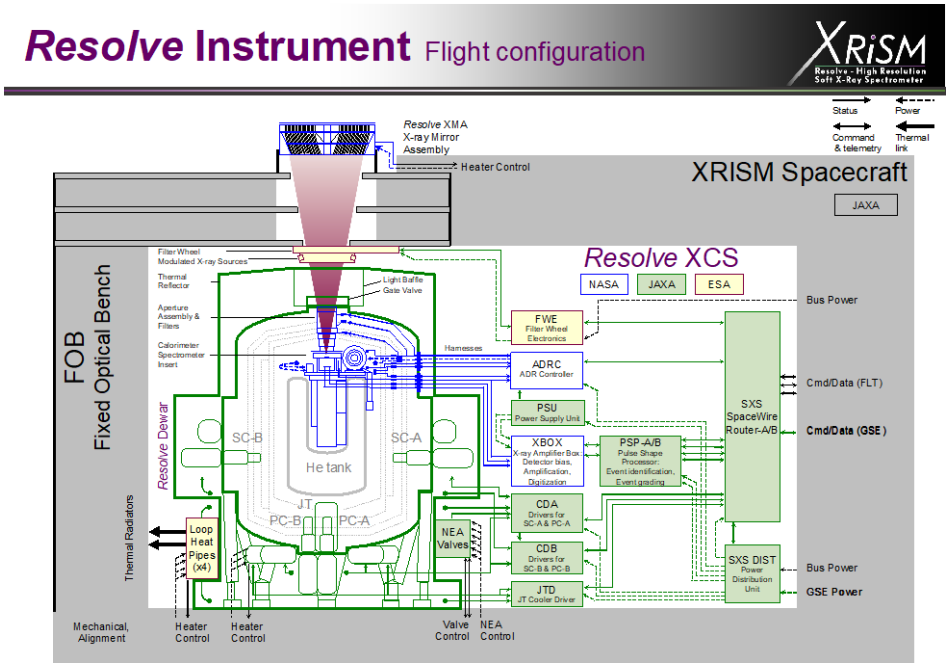

Figure 1. The *Resolve* instrument block diagram depicts the instrument subsystems and their responsible organizations.

All four 2STs are driven at one of 256 sinusoidal frequencies (f_{2ST}) in the 13.933-16.261 Hz range, and the JT is driven at one of 32 sinusoidal frequencies (f_{JT}) in the 50.435-53.826 Hz range. The optimal cooling power corresponds to drive frequencies near the center of the range (~15 Hz for the 2ST and ~52 Hz for the JT). Fortunately *Resolve* had enough margin to permit use of all drive frequencies within the adjustable range. Vibration isolators installed between the DMS and the 2ST compressors[8] intercept most of the exported vibration, but residual vibration propagated inward to the sensitive cryogenic equipment can still cause problems. Following the load path from the cryocoolers mounted to the DMS are 12 Glass Fiber Reinforced Plastic (GFRP) straps suspending the Inner Vapor Cooled Shield (IVCS). From the IVCS 12 Carbon Fiber Reinforced Plastic (CFRP) straps suspend the He tank. A parallel load path goes directly from the DMS to the He tank via continuous fill and vent plumbing lines. The JT shield (JTS), cooled by the JT and its pre-coolers is attached to the CFRP straps between the IVCS and He tank. Finally, the 50 mK components are all suspended by Kevlar within structures mounted to the He tank, and are shaded blue in the Dewar cross section of Figure 2 *(left),* and shown at larger scale in Figure 2 *(right)*.

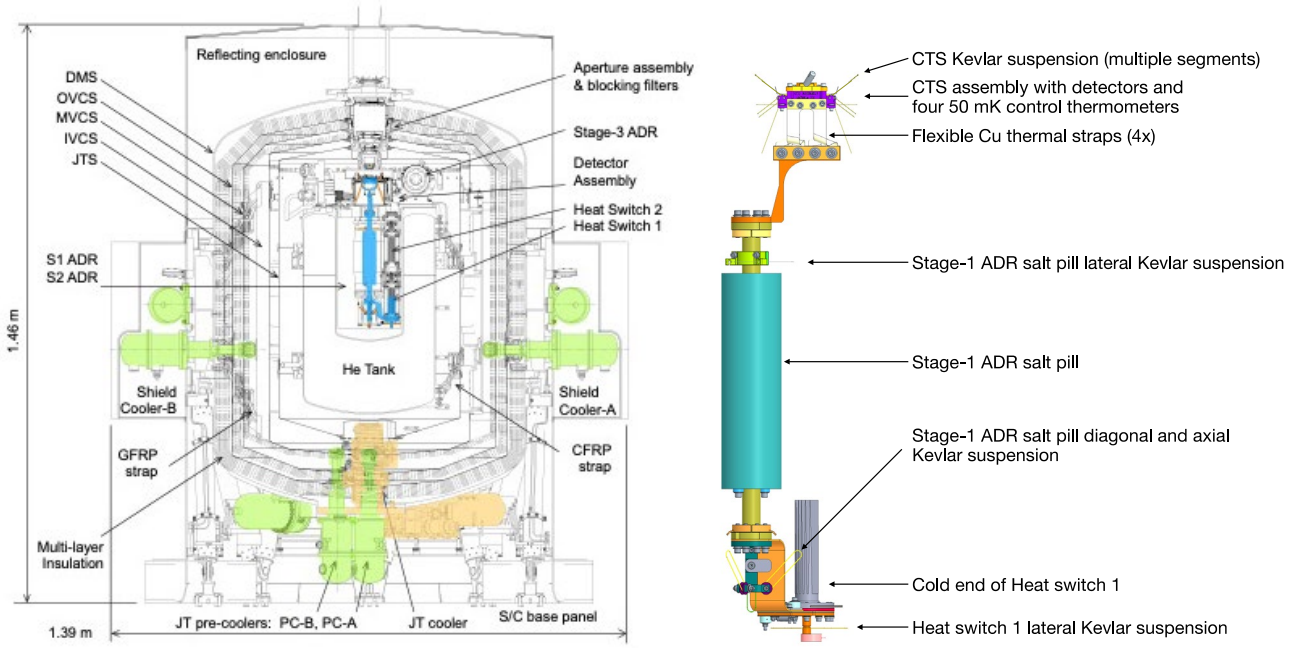

Figure 2. Dewar cross section (left) and components operated at 50 mK (right). The vibration sources are the JT cooler and its two compressors (one shown) located at the bottom center/right of the Dewar (highlighted tan); the two JT pre-coolers (PC-A and PC-B) and their compressors (one shown) located near the JT at the bottom (highlighted green); and the two shield coolers (SC-A and SC-B) and their compressors located on the right and left sides of the Dewar (highlighted green). The hardware most sensitive to micro-vibration are the suspended elements operating at 50 mK (highlighted blue in the center of the Dewar and in the right figure) and its harnessing (not shown).

2. REQUIREMENTS

The primary performance metric for *Resolve* is energy resolution which must be ≤ 7 eV FWHM over the 0.3-12 keV energy range in flight operation. This resolution must be met by the 36-channel detector array in a composite sense, and individually by at least 32 of the 36 calorimeter channels. The energy resolution budget has terms to account for interference from many energy sources (including micro-vibration and electromagnetic), which can be characterized as either noise terms or gain terms. The noise terms represent contributions to the noise in the signal band (~10-200 Hz), and the gain terms represent variations in the signal scaling on an event-to-event time scale . Most terms are incoherent, thus add in quadrature.

Micro-vibration and electromagnetic interference can induce microphonic pickup in detector wiring which manifests as interference noise. An allocation of 1.2 eV (FWHM; i.e. 2.355 x RMS) was included for a single stationary interference tone (regardless of the source), and an allocation of 1.0 eV for unspecified interference. Another 1.0 eV term was allocated to cover the impact of cutting off the signal above 366 Hz to provide immunity to non-stationary, high-frequency interference..

Micro-vibration is also transduced as heat in the cryogenic hardware and causes a real temperature change (or a perceived change if thermometer harnesses move) which degrades temperature control and is therefore captured as a gain term, due to the dependence of the signal amplitude on temperature. The ADRC requirement for 50 mK temperature control is ≤ 2.5 μK RMS, which corresponds to 1.5 eV (FWHM). Low-level vibration that results in heat dissipation in the Kevlar suspension of the Calorimeter Thermal Sink (CTS, the assembly housing the detectors and control thermometers) and is allocated 1 μK RMS, which corresponds to 0.6 eV. Heat dissipated in the Kevlar suspensions of the ADR components will shorten the time that the ADRs can sustain 50 mK control, decreasing observing efficiency. Observing efficiency, defined as the ratio of time that the detectors are stable at 50 mK relative to the full ADR cycle time, must be ≥ 90%.

Measurements of micro-vibration and electromagnetic interference from spacecraft sources were previously reported [9,10]. This paper focuses on mitigation of micro-vibration from *Resolve* sources (JT and Stirling cryocoolers) through a process that led to the identification of the best combination of cryocooler drive frequencies for detector performance.

3. IMPLEMENTATION

Resolve is a rebuild (with minor refinements) of the Soft X-ray Spectrometer (SXS) launched aboard Astro-H/Hitomi[8,11,12,13] in 2016. During testing with the SXS engineering model we learned that a vibration isolation system between the cryocooler compressors and the Dewar was necessary to achieve the required temperature stability at 50 mK ($\leq$ 2.5 μK rms)[14]. Without the vibration isolators temperature stability was severely degraded, in some cases beyond 40 μK rms, resulting in energy resolution of 10 eV or higher. As a result of this experience, and because there are more harmonics of the f_{2ST} within the detector signal band, the number of f_{2ST} steps was increased from 32 to 256. The SXS test program included sampling of the cryocooler parameters while monitoring temperature control and detector noise but only to establish the baseline settings. There were no plans to repeat these tests as it was assumed that nothing would change. However, something did change, and performance was worse after the Dewar vibration test. The cryocooler drive frequencies were updated and performance was improved following a check of performance vs f_{2ST} to choose a new baseline, and then similarly for the f_{JT}.

The SXS experience demonstrated the potential for significant interference from micro-vibration, and a technical risk for micro-vibration was opened at the beginning of the *Resolve* development. A roadmap was prepared which identified opportunities for tests from the earliest possible stage and at each assembly level thereafter to burn down the micro-vibration risk. This paper focuses on the testing that occurred after the Dewar was fully integrated which resulted in the process used to select the cryocooler drive frequencies for *Resolve* after launch.

To operate *Resolve*, its detectors must be at 50 mK, and achieving that requires significant planning, precious execution time, specialized equipment, personnel, and international travel. The overall test program was subdivided into Test Campaigns (TCs) shown in Figure 3. Each TC began with the instrument at room temperature, then continued with cooldown (3-days), post-cooldown hardware checkout and performance trending (2-3 days), special tests (the primary purpose of the TC), and warmup. The early TCs (TC-1 and TC-2) focused on verification of the Dewar and compatibility with the integrated subsystems, TC-3 was for the Dewar cold vibration tests, and TC-4 and TC-5 were dedicated to instrument performance verification and calibration. *Resolve* was delivered to the spacecraft after TC-5, so the remaining TCs (TC-6 through TC-11) were conducted with *Resolve* integrated with the rest of the satellite system. Since *Resolve* was launched cold, TC-11 did not include a warm-up. After launch, *Resolve* was verified and commissioned. Commissioning included running three cryocooler frequency scans leading to the choice of drive frequencies for the science mission.

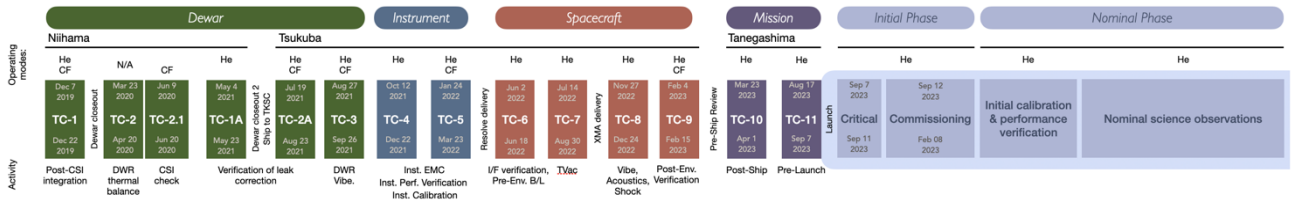

Figure 3. *Resolve* Test Campaigns. This timeline shows (top to bottom) the level of assembly or mission phase, testing location, operating mode (helium mode or cryogen-free mode), TC number with dates and major milestones, and the main purpose of the TC.

4. SEARCH PROCESS

One objective of TC-1 and TC-2 was to verify self-compatibility, part of which was to check detector sensitivity to adjustable cryocooler parameters (f_{JT}; f_{2ST}; relative phase between the 2ST compressors, displacers, and balancers; relative phase between the two JT compressors; different 2ST drive frequencies, and voltage settings of the 2ST balancers). The choice of drive frequency for the JT and 2ST had a significant affect, the phase offset between the two JT compressors did not have a significant affect, and the others were only checked during SXS (all with no affect). In TC-4, sensitivity to cryocooler input power level was also checked, and no significant affect was found. During tests we measured: temperature stability at 50 mK thermometers, changes in ADR magnet current (indicator of heat load change), and detector noise spectra computed by the Pulse Shape Processor (PSP) and separately by non-flight equipment.

With 8,192 possible pairs of operating frequencies (f_{2ST}, f_{2ST}) it was impractical to test all or even a large fraction of the total number of combinations. The goal was to find a stable region at least 3 f_{JT} x 3 f_{2ST} in size. The central pair would become the baseline and trend measurements of the 8 perimeter pairs would serve as an indicator of subtle changes over time. At first, we didn't focus on the search strategy because we assumed finding a stable region would be easy, but it wasn't.

During TC-1 a total of 179 frequency pairs were sampled while looking for a stable region, and no stable regions were found between pairs with interference. Interference was found at 147 frequency pairs with many exhibiting multiple types of interference. The varieties of interference found are:

Increased heat load—When harmonics of the cryocooler drive frequencies align with natural frequencies of suspended 50 mK components heat is dissipated in the Kevlar suspensions (see Figure 2). The ADRC temperature controller compensates for the added heat by decreasing the magnet current to maintain the 50 mK temperature setpoint; when the drive frequency is adjusted away from the resonance, the magnet current recovers. If operated in this condition the extra heat load would reduce the ADRs cooling power, decreasing the instrument observing efficiency. Figure 4 shows the characteristic controller response to two widely spaced temperature setpoint changes and response to a sudden increase in heat load during a frequency scan.

Decreased temperature stability—vibration of the 50 mK thermometers or their lead wires causes rapidly changing sensor resistance (relative to their readout rate of 1 Hz). These fast resistance changes increase the variability of the controlled temperature. Figure 5 shows an example of temperature stability change during a frequency scan.

Low frequencies— The most prevalent form of interference found in TC-1 was low frequency interference which was shown to be beat frequencies caused by small differences between high order harmonics of the two drive frequencies. These frequencies were measured by accelerometers and correlated to detector measurements[15]. Evidence of low frequency interference can be identified in detector noise spectra computed on-board in the PSP for downlink. See example in Figure 6 (a).

Microphonic pickup— the detectors' fine lead wires are tensioned to around 2 kHz, and these tensioned leads are extremely sensitive to microphonic pickup. Vibration induces very small voltage changes which are amplified along with the detector signal. This interference can affect a single channel, groups of channels, or the entire array and is also observable in detector noise spectra. See example in Figure 6 (b).

Channel resonances—Each individual pixel has several high frequency resonances beginning around 1 kHz. Some channel resonance frequencies were noted during testing and found to be coincident with high-order harmonics of one of the cryocoolers (e.g., Ch. 23 resonance was noted at 1233 Hz while the f_{JT}=53.594 Hz and f_{2ST}=15.636 Hz. The corresponding harmonics were: JT 23rd harmonic = 1233 Hz and 2ST 79th harmonic = 1235 Hz). In cases like these, the channel will ring causing false triggers that fill data buffers and render the channel useless. Moving just one drive frequency step eliminated the interference. See example in Figure 6 (c).

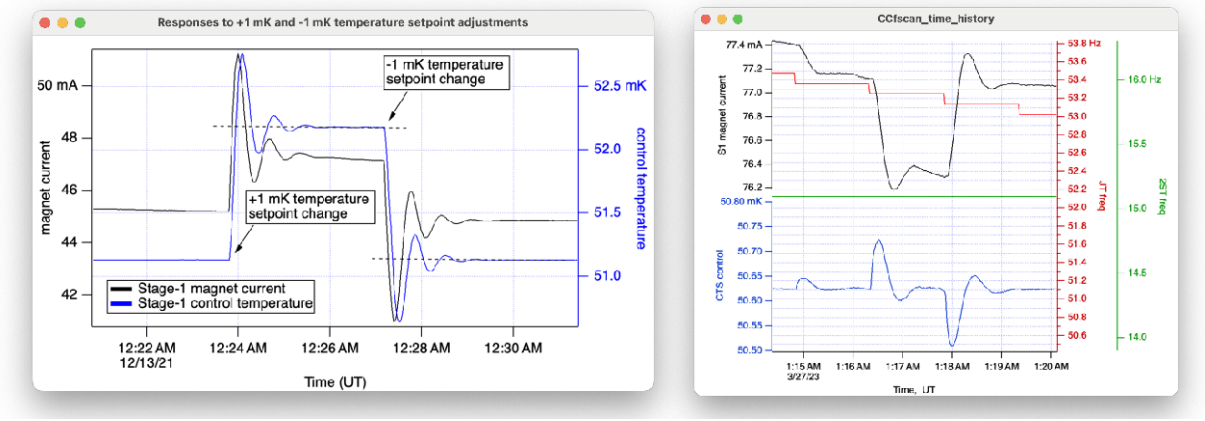

Figure 4. ADR controller responses. Plotted on the left is an example where the temperature setpoint was increased by +1 mK and back a few minutes later. When the setpoint was changed, the controller increased magnet current to raise the temperature, and vice versa when the setpoint was lowered. Note that the magnet current and temperature responded with the same polarity. The plot on the right shows a portion of a f_{JT} scan where a suspension resonance was excited by a harmonic of the JT drive frequency when it was switched to 53.25 Hz. The resonance deposits heat into the Kevlar driving up the temperature, and in response the controller decreases magnet current to compensate for the higher temperature. Note here that magnet current and temperature respond with opposite polarity which is consistent with an external stimulus. In both cases the settling time is on the order of one minute.

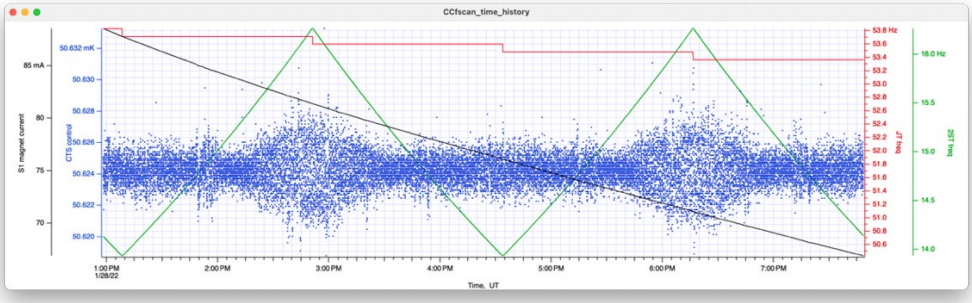

Figure 5. Change in temperature stability as a function of the f_{2ST}. In this example the scatter of temperature readings (blue) shows how temperature stability changes during a sweep of the f_{2ST}. The best stability here (f_{2ST} ~14.7 Hz) was 0.6 μK RMS while the worst (f_{2ST} ~16 Hz) was about 2 μK RMS.

Figure 6. Examples of interference: a) low frequency interference detected using non-flight equipment; b) microphonic pickup on all channels across the signal band; c) channel resonance identified in the detector noise spectrum (top) and ringing shown in the time-domain (bottom); d) harmonics of the JT within the signal band (the detectors were at 1K- where they are much less sensitive).

With so many instances of interference it was more difficult that expected to find a stable region. A search strategy was needed to efficiently reduce the number of candidates and select a baseline in a reasonable amount of time. The challenge was to strike the right balance between measurement sensitivity (generally longer measurements) and overall test duration. The descriptions below summarize our approach and a few of the pivotal lessons and changes along the way.

Scans of the f_{2ST} and f_{JT} began in TC-4, and helped locate a stable region around f_{2ST} =14.63 Hz and f_{JT} = 51.89 Hz where the temperature stability was 0.64 μK RMS and the detector noise spectrum was free of interference. That same region was re-checked in the TC-5 trend test, but the whole region had changed dramatically and temperature stability at the baseline pair became 4.41 μK RMS and similar at the surrounding pairs.

A new baseline for TC-5 was needed urgently to proceed with performance verification and calibration, so we repeated the f_{JT} scan and selected the best 6 contiguous frequencies and repeated the f_{2ST} scan and selected the best 26 contiguous frequencies. Then during one overnight test, we scanned the 156 intersecting frequency pairs and collected detector noise spectra at each setting. The best of the group was selected as the baseline, but all 156 pairs suffered from some JT*3 and JT*4 harmonic frequency interference. We concluded that the screening process had been too aggressive which led to a candidate region for the final noise scan that was so small that all pairs were affected by the same interference. We reasoned that greater separation, or diversity, among candidate frequency pairs would lead to a greater likelihood of finding a noise-free solution.

In addition to vibration changing interference dependency on cryocooler frequencies (a lesson from SXS), we had new evidence that Dewar thermal cycles also changed the interference pattern. That meant that frequency scans would be needed in the other TC's and also after launch. Figure 7 shows the frequencies associated with heat load increases during the TC-4 and TC-5 f_{JT} scans.

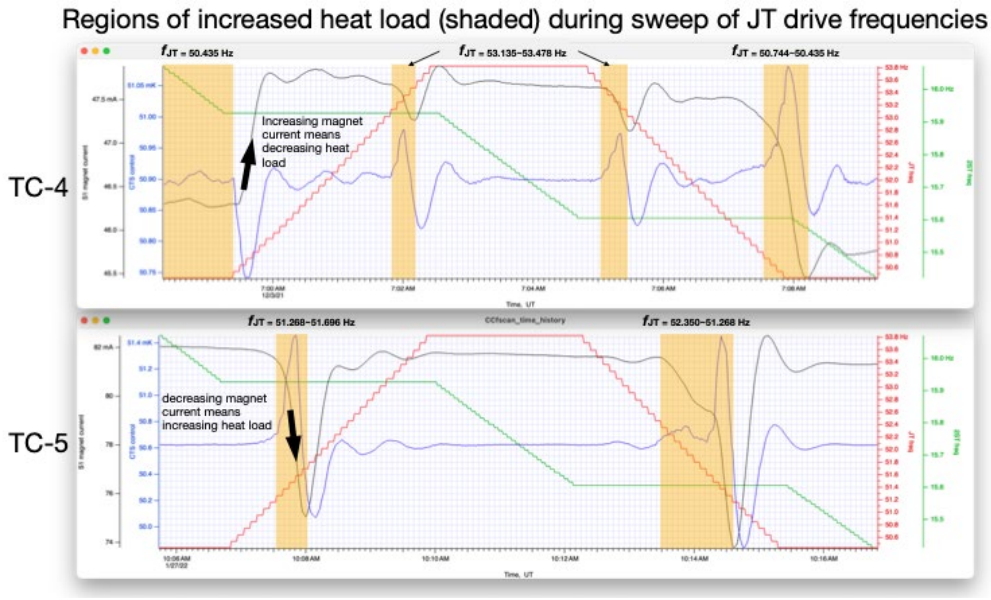

Figure 7. Two scans of the f_{JT} with significantly different results in two test campaigns, separated only by warming the Dewar to room temperature and re-cooling the Dewar to operational temperature. The shaded regions and noted frequencies show where heat loads were significantly higher. Each interference highlighted range begins when the magnet current (black curve) started decreasing and ends when the magnet current reaches its minimum.

After TC-5, only minor refinements were made to measurement integration times to improve effectiveness and to procedural structures to make them compatible with flight operations. Beginning in TC-6, the frequency scans were run from procedures that accommodated flight operational constraints such as the maximum number of commands, data recorder allocation, and durations of uninterrupted time at 50 mK. These constraints were not necessary during ground testing but including them in the tests contributed to successful execution during commissioning.

The final suite of frequency scans became:

> **f_{JT} scan**: scan all 32 f_{JT} (at any f_{2ST}) in both directions, integrating for 90 seconds at each frequency; choose two consecutive f_{JT} for the f_{2ST} scan and the 12 best f_{JT} for the noise scan based on 50 mK thermometry and change in ADR magnet current. The runtime was 1 hour, 33 minutes.
>
> **f_{2ST} scan**: scan all 256 f_{2ST} at the two selected f_{JT}, integrating for 24 seconds at each frequency; choose the best 120 f_{2ST} as either one contiguous group of 120, or two groups of 60. The runtime was 1 hour, 46 minutes.
>
> **Noise scan**: scan the resulting 1,440 frequency pairs, integrating for 60 seconds at each pair; rank the pairs based on detector noise criteria and temperature stability to select a baseline and alternates. The total runtime was 26 hours, 30 minutes, and divided into six equal parts.

5. RESULTS

The in-orbit commissioning of *Resolve*[16] began a month after its September 7, 2023 launch and completed in February 2024. The three frequency scans started shortly after reaching 50 mK for the first time and were completed within three weeks with no issues. The scans were all conducted away from the South Atlantic Anomaly (SAA) where a high rate of particle hits on the thermometers disturbs the stability (consequently, these time periods are excluded from the nominal science data sets). The runtime of the f_{JT} and f_{2ST} scans were each less than 2 hours making them relatively easy to schedule. The runtime for the noise scan was longer than the intervals between SAA crossings and the data volume of the noise spectra generated on-board in the PSP was larger than what could be downlinked in a day. As a result, this scan was divided into six equal parts of 4 hours 25 minutes each. They were executed in orbits away from the SAA on six

consecutive days to manage the large data volume to downlink each day. Once the results were analyzed the final drive frequencies were selected and changed by command on Nov. 3, 2024. To date, performance remains stable with no indication of change.

Figure 8 shows the three-step process of narrowing the 8,192 frequency pair combinations to one, and Figure 9 shows the timeline and context of the measurements. A one-dimensional scan of the f_{JT} was run first to eliminate interference caused by the JT by narrowing the JT candidate frequencies. Another one-dimensional scan of the f_{2ST} was run next to eliminate interference caused by the 2ST by narrowing the 2ST candidate frequencies. Any remaining interference was eliminated in data analysis and ranking of the detector noise spectra collected in a two-dimensional scan of the 1,440 remaining candidates after the first two scans.

Figures 10 and 11 compare the results of the f_{JT} and f_{2ST} scans during ground testing, TC-4 through TC-10, and in-orbit during commissioning.

Figure 8. A summary of the 3-step scan process plotted on a rectangular space representing the 256 2ST x 32 JT frequencies. Green highlight indicates the results of each scan.

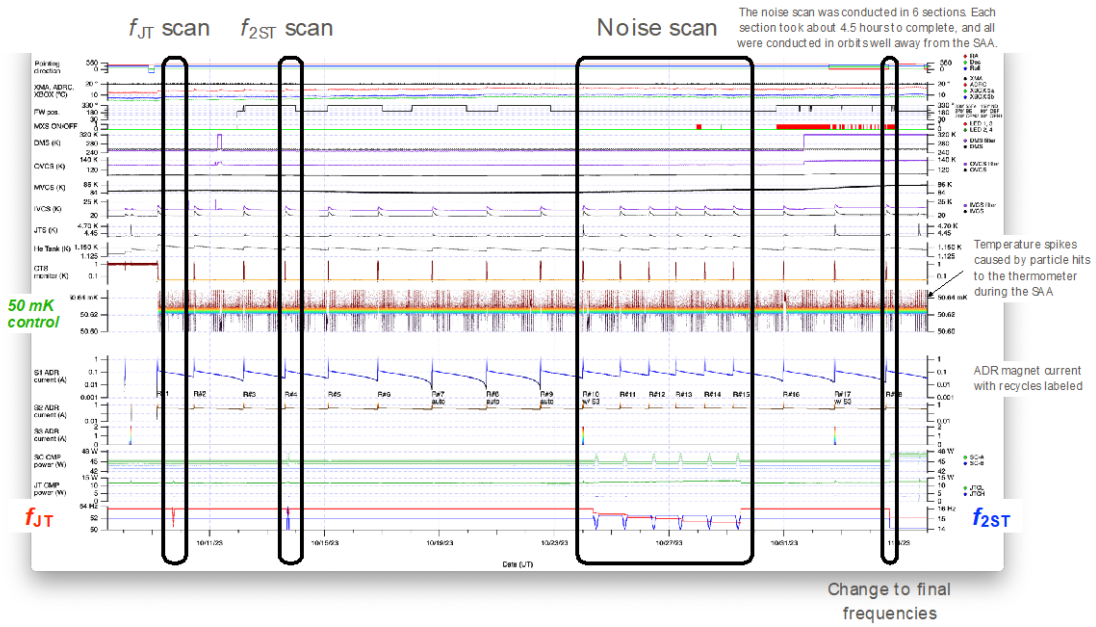

Figure 9. Timeline and context of the cryocooler frequency scans during commissioning

	Pre-TVac	TVac 1	TVac 2							
	TC-4	TC-5	TC-6	TC-7	TC-7	TC-7	TC-8	TC-9	TC-10	Flight	f_{JT}, Hz
	15	3	1	8	5	7	1	2	13	29	53.826
	24	2	2	3	4	6	15	1	15	32	53.710
	25	4	24	17	1	19	14	5	5	25	53.594
	17	1	14	15	12	21	17	13	29	17	53.478
	23	6	22	SKIP	23	18	16	32	30	10	53.363
	22	7	27	SKIP	11	11	18	24	32	3	53.249
	20	8	28	SKIP	10	17	9	25	31	14	53.135
	18	5	20	SKIP	6	22	12	14	6	15	53.021
	21	9	26	6	2	1	8	10	21	11	52.908
	19	10	25	10	2	15	10	18	18	7	52.796
	14	11	15	9	3	25	4	21	11	4	52.683
	11	12	16	8	27	4	12	26	14	9	52.572
	13	13	22	13	16	8	2	3	8	23	52.461
	9	15	23	1	17	16	30	16	13	28	52.350
	2	16	17	SKIP	8	3	26	22	3	16	52.240
	5	17	18	SKIP	14	23	29	31	2	1	52.130
	6	21	29	SKIP	19	10	28	30	17	5	52.021
	7	22	31	SKIP	26	14	21	15	20	18	51.912
	1	25	32	SKIP	21	14	24	20	9	8	51.804
	4	24	30	SKIP	13	5	20	19	24	21	51.696
	8	29	19	21	20	14	25	29	28	12	51.588
	12	32	11	19	23	24	27	23	19	6	51.481
	10	31	8	22	24	9	8	29	23	9	51.375
	3	30	7	20	9	9	31	7	22	19	51.268
	16	23	6	18	19	21	23	4	16	13	51.163
	26	27	5	16	15	26	9	10	10	20	51.057
	27	28	4	12	25	27	6	13	10	24	50.953
	31	26	9	5	32	28	14	27	1	22	50.848
	30	20	13	5	30	30	5	13	9	27	50.744
	29	14	12	3	29	32	32	10	25	26	50.641
	29	19	11	11	31	31	23	9	27	30	50.537
	32	18	3	14	28	29	20	17	26	31	50.435
Integration time at each setting	6 s	6 s	6 s	60 s	90 s	90 s	90 s	90 s	90 s	90 s	
	6 s	6 s	6 s	60 s	90 s	90 s	90 s	90 s	90 s	90 s	
Avg. temp stability, μK RMS	67.8	361.4	11.9	4.3	7.1	7.3	5.1	4.7	15.5	1.4	

Figure 10. Ranked temperature stability trend of the f_{JT} scans. One surprising and clear conclusion is that there is no discernable pattern from one test campaign to another. This is evident in both the rank numbers (yellow=best, black=worst) of each frequency and in the variability among the average temperature stability at all measured frequencies. During TC-7, the test campaign for the spacecraft thermal vacuum test (TVac), the f_{JT} scan was run three times, once at ambient pressure before closing the vacuum chamber, and twice in TVac during different cold cases. The difference between the Pre-TVac result and the two TVac results may be attributed to removal of atmospheric pressure from the Dewar, and/or due to the decreased temperature of the Dewar. But importantly, the similar results in the latter two cases give confidence that once the internal and external environments have stabilized the results will be stable over time. The in-orbit scan showed regions of large interference at the high and low frequencies with better performance in the mid-frequencies, continuing to defy any consistent trend.

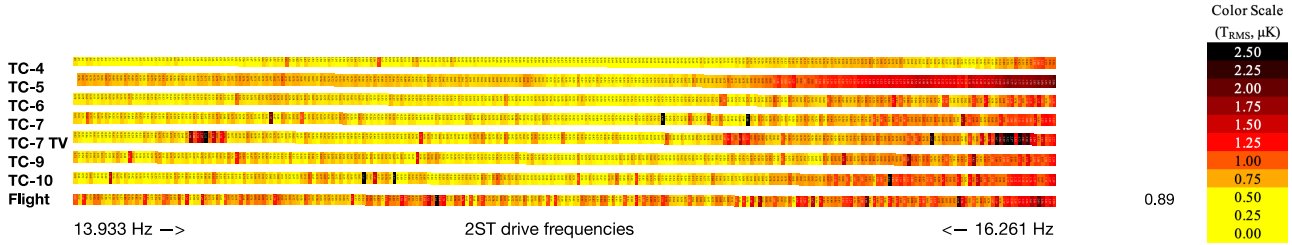

Figure 11. Temperature stability trend of the f_{2ST} scans. Unlike the f_{JT} scans, most f_{2ST} scans (other than TC-7 TVac) showed few signs of significant interference and a general trend towards worse performance at higher frequencies and slightly better performance at mid-range frequencies. The scan in-orbit showed slightly worse stability overall but remained consistent with the general trend of the ground tests.

Once the data from the noise scan was downlinked, the noise spectra were sorted and grouped by channel number, aka pixel. Figure 12 a) shows an example of all noise spectra for one channel plotted together where color represents a different pair of drive frequencies. Then criteria were established (~50 criteria) such as the low frequency limits shown in Figure 12 b). The automated analysis flagged spectra with criteria violations corresponding to a variety of different interference types, like the examples shown in Figures 12 c), d), and e). The results are shown on plot of drive frequencies, color coded by the number of criteria violations for each frequency pair (Figure 12 f). This analysis reduced the number of candidates to 180, each with ≤ 7 criteria violations. The remaining candidates were assessed individually and scored. The final choice among the best performing candidates (blue markers in Figure 13 a) also considered temperature stability (Figure 13 b) and performance at neighboring frequency pairs. The noise spectra, Figures 13 c) and d), are for the default frequency pair and the selected frequency pair, respectively. The result has minimal interference in the signal band (below 200 Hz) and excellent sub-micro Kelvin temperature stability.

Figure 12. Automated noise spectra analysis. a) all noise spectra are combined by channel; b) approximately 50 criteria are established, this example shows the low-frequency limit; c), d), and e) are examples of removing different types of interference: mid-band affecting all channels, low frequency affecting multiple channels, and channel resonance, respectively; and f) shows a map of the results, narrowed to 180 candidates to be individually assessed.

Figure 13. Final selection maps and noise spectrum: a) shows a map of the final evaluation. Small markers on the graph represent candidates eliminated in the automated analysis. Large markers are the 180 remaining candidates that were inspected and ranked by color (blue= best, green= worst); b) temperature stability was also considered in the final ranking; c) the detector noise spectrum of the default frequency pair taken in-orbit before switching to the newly selected frequencies; d) the detector noise spectrum of the selected frequency pair.

6. CONCLUSIONS AND LESSONS

The cryocooler drive frequency scan process efficiently reduced 8,192 possible configurations to a single performance optimized solution for the *Resolve* science mission.

Testing revealed five different types of interference caused by micro-vibration from the cryocoolers, and an efficient search method was developed to measure interference as a function of the two cryocooler drive frequencies.

The JT cryocooler drive frequency affected temperature stability the most and had the least repeatable results. The JT drive frequencies that caused interference and the magnitude of the interference changed every time the Dewar was warmed and cooled between ground test campaigns though the Dewar configuration did not change. The Stirling cryocooler drive frequencies also caused interference, but with smaller variability and greater repeatability than the JT. Other interference was eliminated in analysis of detector noise spectra from the noise scan before making the final choice of cryocooler drive frequencies.

Resolve was a re-build, which is not common for astronomical telescopes, and that enabled the team to start the project with the experience of having worked through the issues of the prior build. That doesn't mean that the new build will have the same issues, but it does sensitize the team to the most likely challenges. *Resolve* started with the knowledge that micro-vibration was a serious technical risk and began managing that risk from the very beginning. Yet the cryocooler drive electronics design with its selectable drive frequencies predated any knowledge of how interference from micro-vibration would manifest. Some might argue that designs shouldn't include too many configurable options as they will translate to burdensome testing. But there are surprises on every mission, even on re-builds. It turns out that for *Resolve* the configurable settings were necessary to overcome the surprisingly unpredictable interference caused by micro-vibration.

REFERENCES:

[1] Tashiro, M., et al., “Status of x-ray imaging and spectroscopy mission (XRISM),” Proceedings of SPIE, Volume 11444, id. 1144422 (December 2020); https://doi.org/10.1117/12.2565812

[2] Kelley, R., et al., “Overview and Inflight Performance of the Resolve High-Resolution Soft X-Ray Spectrometer on the X-Ray Imaging and Spectroscopy Mission,” Proc. SPIE, this issue.

[3] Porter, F.S., et al., “In-Flight Performance of the XRISM/Resolve Detector System,” Proc. SPIE, this issue.

[4] Shirron, P., et al., “On-orbit performance of the Adiabatic Demagnetization Refrigerator on XRISM,” Proc. SPIE, this issue.

[5] Chiao, M., et al., “Design and Performance of the Hitomi/XRISM Adiabatic Demagnetization Refrigerator Controller," Proc. SPIE, this issue.

[6] Chiao, M., et al., “System design and implementation of the detector assembly of the Astro-H soft X-ray spectrometer,” Proceedings of SPIE 9905, 99053M (2016); https://doi.org/10.1117/12.2231897

[7] Yoshida, S., et al., “Performance test results of a helium Dewar for the Resolve instrument aboard the XRISM,” Cryogenics, Volume 139 (April 2024); https://doi.org/10.1016/j.cryogenics.2024.103831

[8] Ishisaki, Y., et al., "Status of Resolve instrument onboard x-ray imaging and spectroscopy mission (XRISM)”, Proceedings of SPIE, Volume 12181, id 121811S, (2022); https://doi.org/10.1117/12.2630654

[9] Hasebe, T., et al., “Ground test results of the microvibration interference for the x-ray microcalorimeter onboard x-ray imaging and spectroscopy mission, ” Journal of Astronomical Telescopes, Instruments, and Systems, Vol. 9, Issue 1, 014003 (March 2023); https://doi.org/10.1117/1.JATIS.9.1.014003

[10] Kurihara, M., et al., “Ground test results of the electromagnetic interference for the x-ray microcalorimeter onboard XRISM, ” Journal of Astronomical Telescopes, Instruments, and Systems, Vol. 9, Issue 1, 018004 (March 2023); https://doi.org/10.1117/1.JATIS.9.1.018004

[11] Takahashi, T., “Hitomi (ASTRO-H) x-ray astronomy satellite,” J. of Astronomical Telescopes, Instruments and Systems, 4 021402 (2018). https://doi.org/10.1117/1.JATIS.4.2.021402

[12] Kelley, R. L., et al., “The Astro-H high resolution soft x-ray spectrometer,” Proceedings of SPIE 9905, 99050V (2016); https://doi.org/10.1117/12.2232509

[13] Mitsuda, K., et al., “Soft x-ray spectrometer (SXS): the high-resolution cryogenic spectrometer onboard ASTRO-H,” Proceedings of SPIE 9144, 91442A (2014); https://doi.org/10.1117/12.2057199

[14] Takei, Y., et al., “Vibration isolation system for cryocoolers of soft x-ray spectrometer on-board ASTRO-H (Hitomi),” Journal of Astronomical Telescopes, Instruments, and Systems, Vol. 4, Issue 1, 011216 (February 2018); https://doi.org/10.1117/1.JATIS.4.1.011216

[15] Imamura, R., et al., “Mechanical cryocooler noise observed in the ground testing of the Resolve X-ray microcalorimeter onboard XRISM,” J. Low Temp Phys 211, 426-433 (2023); https://doi.org/10.1007/s10909-022-02935-1

[16] Maeda, Y., et al., “In-orbit operation of Resolve,” Proc. SPIE, this issue.